Specific Interaction of Camptothecin, a Topoisomerase I Inhibitor, with Guanine Residues of DNA Detected by Photoactivation at 365 nm

F. Leteurtre, M. Fesen, G. Kohlhagen, K. W. Kohn, and Y. Pommier*

Laboratory of Molecular Pharmacology, Developmental Therapeutics Program, Division of Cancer Treatment, National Cancer Institute, National Institutes of Health, Bethesda, Maryland 20892

Received February 22, 1993; Revised Manuscript Received June 8, 1993

ABSTRACT: Camptothecin-induced DNA photolesions were examined after UVA irradiation at 365 nm. DNA single-strand breaks were induced both in supercoiled and in relaxed SV40 DNA. In uniquely end-labeled human c-myc DNA, camptothecin-induced cleavage occurred exclusively at guanines and was markedly enhanced by hot piperidine treatment. Runs of polyguanines were the most cleaved, especially in their 5′ flank. Primer extension experiments in the absence of piperidine treatment confirmed these results and did not show additional lesions. We found that synthetic single-stranded oligonucleotides were more reactive than duplex oligonucleotides. In addition, an excess of dideoxyguanosine triphosphates competed for camptothecin-induced DNA photolesions. Therefore, camptothecin stacking in DNA grooves is more likely than genuine drug intercalation. Groove shielding with sodium or magnesium reduced camptothecin-induced photodamage while minor groove occupancy with spermine extended damages. Photolesion mechanisms were investigated using scavengers. In aerobic conditions, the most effective scavengers were thiourea, sodium azide, and catalase. Protection by superoxide dismutase was weak, and mannitol was ineffective. In anaerobic conditions, lesions were more extensive. Taken together, these results show that photoactivated camptothecin interacts specifically and intimately with guanines. This finding is consistent with preferential stimulation of topoisomerase I cleavage at sites that bear a guanine at their 5′-DNA terminus [Jaxel, C., et al. (1991) *J. Biol. Chem.* 266, 1465–1469] and with the camptothecin stacking model at topoisomerase I DNA cleavage sites.

DNA topoisomerases are nuclear enzymes involved in the control of DNA topology. Type 1 topoisomerase (topl)[1] induces DNA single-strand breaks, while the type 2 enzyme (top2) catalyzes double-strand cuts. In either case, DNA cleavage results from transesterification reactions from a DNA backbone phosphate to an enzyme tyrosine residue. Phosphotyrosine linkage is with the 3′-DNA terminus for topl and with the 5′ termini for top2. Passage of a DNA single- or a double-strand through the DNA cleavage site changes the DNA linking number in steps of one or two (topl and top2, respectively) (Adamovics et al., 1979; Huff et al., 1989). A variety of topl and top2 inhibitors act as enzyme poisons by stabilizing the cleavable complex intermediary product which can be seen experimentally by the addition of detergent and proteinase K. Camptothecin (CPT) is a specific topl inhibitor, while *m*-AMSA, doxorubicin, ellipticine, mitoxantrone, and epipodophyllotoxin derivatives are top2 poisons (Liu, 1989; Pommier & Kohn, 1989; Pommier & Tanizawa, 1993).

Topoisomerase cleavages in the presence of inhibitors exhibit, on naked DNA, a strong preference for one base immediately flanking the cleavage site either at the 3′ terminus of the break (position −1) or at the 5′ terminus (position +1). Preferential bases are guanine (G) +1 for camptothecin (CPT) (Jaxel et al., 1991), adenine (A) +1 for *m*-AMSA (Pommier et al., 1991), A(−1) for adriamycin (Capranico et al., 1990), cytosine(−1) for epipodophyllotoxins (Pommier et al., 1991) and mitoxantrone (unpublished result), and thymine(−1) for ellipticine (Fosse et al., 1991). These observations have led to a hypothesis that specific stacking interactions occur between drugs and the preferred bases at the topoisomerase cleavage site (Jaxel et al., 1991; Pommier & Tanizawa, 1993). Although such stacking seems obvious for DNA intercalators, it might also be possible for nonintercalators, such as CPT because of its nearly planar aromatic structure. According to our stacking model, CPT might have a preferential affinity for guanines.

Binding studies of CPT indicate that the drug affinity is much greater for topl–DNA complexes than for purified DNA (Hertzberg et al., 1989a, 1990). Nevertheless, low-affinity CPT binding has been demonstrated with AT-rich DNA at low salt concentrations as well as higher affinity binding to GC-rich regions at high salt concentrations (Fukada, 1985). Because of the lability of these CPT–DNA interactions in the absence of topl, we attempted to stabilize the CPT–DNA complexes using photoactivation. Photoactivation is a potent technique to freeze molecular interactions. Photons can activate molecules with delocalized π electrons. The increased energy generates reactive radicals which react with other molecules. Drug photoactivation in the immediate vicinity of DNA can generate photoadducts and/or DNA cleavage. Photoadditions have been demonstrated with psoralen at T (Sage et al., 1989; Sage & Moustacchi, 1987) or with aflatoxin at G (Shaulsky et al., 1990). DNA cleavage has been shown with the antitumor antibiotic dynemicin A at purines (Shiraki & Sigiura, 1990). Because CPT has been shown to be photoactivable at 365 nm and to induce DNA cleavage under these conditions (Hertzberg et al., 1989a; Kuwahara et al., 1986; Lown & Chen, 1980), we hypothesized that photoactivation of a CPT molecule in contact with a specific DNA base should provide a detectable signal using DNA sequencing methodology and provide evidence for a sequence-selective interaction of CPT with DNA.

* To whom correspondence should be addressed at Building 37, Room 5C25, National Institutes of Health, Bethesda, MD 20892. Telephone: 301-496-5944. Fax: 301-402-0752.

[1] Abbreviations: CPT, (20*S*)-camptothecin; G, guanine; *m*-AMSA, 4′-(9-acridinylamino)methanesulfon-*m*-anisidide; PCR, polymerase chain reaction; topl, DNA topoisomerase I.

Our results demonstrate the specific interaction of photoactivated CPT with guanines. They are consistent with the preferential stimulation of topl cleavage at topl sites with G+1.

MATERIALS AND METHODS

Drugs, Enzymes, and Chemicals. (20*S*)-Camptothecin (CPT) and derivatives were obtained from the Drug Synthesis and Chemistry Branch, National Cancer Institute, Bethesda, MD. Drug stock solutions were made in dimethyl sulfoxide at 10 mM, and aliquots were stored at −70 °C. Further dilutions were made in distilled water immediately before use.

Calf thymus topl, T4 polynucleotide kinase, terminal transferase, Taq DNA polymerase, agarose, and polyacrylamide/bis were purchased from Perkin Elmer Cetus (Norwalk, CT), Gibco Bethesda Research Laboratories (Gaithersburg, MD), or New England Biolabs (Beverly, MA). [γ-^{32}P]ATP and [α-^{32}P]cordycepin were purchased from New England Nuclear Research Products (Boston, MA). Bovine liver catalase and bovine erythrocyte superoxide dismutase were purchased from Sigma (St. Louis, MO).

DNA Substrates and Preparation of End-Labeled DNA Fragments. Simian virus 40 (SV40), c-myc human DNA inserted in pBR322, and oligonucleotides were purchased from Gibco BRL, from the American Type Culture Collection (Rockville, MD), and from the Midland Certified Reagent Co. (Midland, TX), respectively.

The 254 base pair DNA fragment from the human c-myc first intron was prepared by PCR using the two primers: 5′-^{32}P-GTAATCCAGAACTGGATCGG-3′ sense primer starting at 3035 and 5′-ATGCGGTCCCTACTCCAAGG-3′ antisense primer starting at 3288, with the numbers referring to the genomic position of the corresponding base in c-myc DNA. Single-end-labeling was obtained by ^{32}P-5′-end-labeling. Ten picomoles of DNA was incubated for 30 min at 37 °C with 10 units of T4 polynucleotide kinase and 10 pmol of [γ-^{32}P]ATP (100 μCi) in kinase buffer (70 mM Tris-HCl, pH 7.6, 0.1 M KCl, 10 mM $MgCl_2$, 5 mM dithiothreitol, and 0.5 mg/mL bovine serum albumin). Reactions were stopped by adding EDTA (ethylenedinitrilotetraacetic acid) to a final concentration of 30 mM, and heat denaturation at 70 °C for 15 min. After ethanol precipitation, labeled oligonucleotides were resuspended in water and used for PCR. Approximately 0.1 μg of the c-myc plasmid that had been restricted by *Xba*I and *Pvu*II enzymes was used as template during the PCR. Ten picomoles of each primer, 1 of them labeled, was used in 16 temperature cycle reactions (each cycle with 93 °C for 1 min, 56 °C for 1 min, and 72 °C for 2 min). The last extension was for 10 min. DNA was purified using PrimeErase columns (Stratagene) and ethanol precipitation. The resulting 254 base pair PCR fragment corresponds to the human c-myc DNA region between positions 3035 and 3288 with labeling at 3035, according to the GenBank numbers.

The 30-mer oligonucleotides used directly for CPT–UV reactions and corresponding to a strong camptothecin-inducible topl cleavage site in SV40 DNA (Jaxel et al., 1991) are shown in Figure 6. End-labeling was performed either at the 3′ or at the 5′ termini using single-stranded oligonucleotides. 5′-End-labeling was performed as described above. 3′-End-labeling was performed using 10 pmol of oligonucleotide, 36 units of terminal deoxynucleotide transferase, and 20 pmol of [α-^{32}P]cordycepin (100 μCi) in 35 μL of reaction buffer containing 100 mM sodium cacodylate, pH 7.2, 0.1 mM dithiothreitol, and 10 mM $MgCl_2$ for 1 h at 37 °C. Reactions were stopped by adding 30 mM EDTA (final concentration). Purification was done using Strataclean resin (Stratagene, La Jolla, CA) and G-50 columns (Boehringer Mannheim, Indianapolis, IN). Labeled DNA was either used single-stranded or used after annealing with the unlabeled complementary oligonucleotide. Annealing was performed by mixing equal amounts of each complementary strand in 80 μL of annealing buffer (10 mM Tris-HCl, pH 7.8, 100 mM NaCl, and 1 mM EDTA). The reaction mixture was heated to 65 °C for 5 min and left at room temperature until cooling to 20 °C.

DNA Photocleavage Reactions. Labeled DNA fragments (approximately 0.1 pmol) were equilibrated with or without CPT in 20 μL of buffer (25 mM Tris-HCl, pH 7.5, 150 mM KCl, and 0.1 mM EDTA). UV irradiation at 365 nm (20–30 J m^{-2} s^{-1}) was performed at room temperature through a water screen to trap infrared wavelengths and reduce evaporation. After irradiation, samples were ethanol-precipitated. When indicated, piperidine treatments were performed according to Maxam and Gilbert (1980) by adding 100 μL of an aqueous 1 M piperidine solution and heating of the samples to 90 °C for 20 min. Piperidine was removed by lyophilization followed by two washes with 20 μL of water and evaporation.

In oxygen-free experiments, samples were placed inside a balloon, vacuum was applied, and air was replaced by argon. The operation was repeated 10 times before sealing of the balloon and UV irradiation.

Photolesion Detection by Primer Extension. One-tenth microgram of the 254 bp unlabeled DNA fragment prepared as above by PCR was reacted with CPT–UV and ethanol-precipitated. CPT-induced photolesions were detected by primer extension using the 5′-labeled primer starting at 3288 (the antisense primer). Conditions used were as for a 1 PCR cycle. Stop point positions were identified by comparison with a Sanger reaction using dideoxynucleotides.

Electrophoresis. For agarose gel analysis, 3 μL (10×) of loading buffer (0.3% bromophenol blue, 16% Ficoll, and 10 mM Na_2HPO_4) was added to the samples which were loaded into 1.2% agarose gels made in (1×) TBE buffer (89 mM Tris, pH 8, 89 mM boric acid, and 2 mM EDTA). To allow the separation of supercoiled, relaxed, and nicked DNA, the gel was run at 2 V/cm overnight in the presence of 1 μM ethidium bromide. The DNA was visualized under UV light and photographed with Polaroid type 55 films. Film negatives were scanned using a Beckman DU-8B spectrophotometer coupled with a computer for quantitation of DNA peaks (Jaxel et al., 1989).

For DNA sequence analysis, samples were precipitated with ethanol and resuspended in 2.5 μL of loading buffer (80% formamide, 10 mM NaOH, 1 mM EDTA, 0.1% xylene cyanol, and 0.1% bromophenol blue). Samples were heated to 90 °C and immediately loaded into DNA sequencing gels [6–8% polyacrylamide with an acrylamide:bis(acrylamide) ratio of 19:1; or 16% polyacrylamide with an acrylamide:bis(acrylamide) ratio of 110:1] containing 7 M urea in (1×) TBE buffer. Electrophoresis was at 2500 V (60 W) for 4 h. Gels were dried on 3MM paper sheets and autoradiographed with Kodak XAR-2 film.

RESULTS

UV Irradiation at 365 nm Induces DNA Cleavage in the Presence of CPT. Supercoiled (Sc) or topl-relaxed (R) SV40 DNA was used to assay DNA cleavage by conversion from the closed circular forms to the nickel (N) and linear (L) forms. Agarose gel electrophoresis run in the presence of 1 μM ethidium bromide was used to separate the four forms.

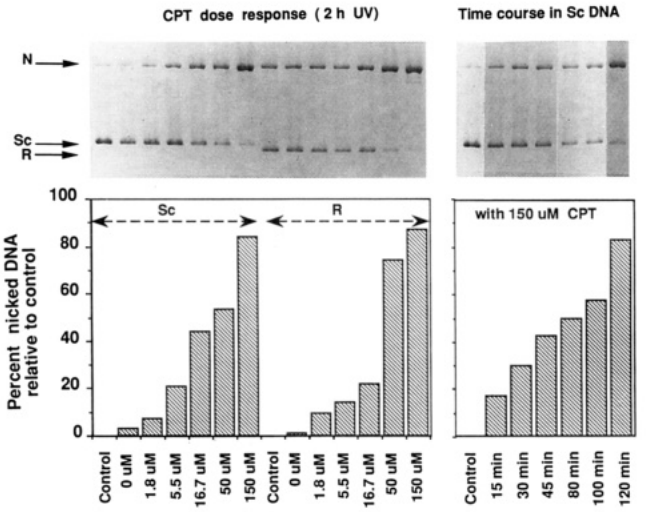

FIGURE 1: Camptothecin-induced DNA cleavage by photoactivation at 365 nm. 0.4 μg of supercoiled (Sc) or relaxed (R) SV40 DNA was irradiated at 365 nm, either for 2 h with increasing CPT concentrations (left panels) or with 150 μM CPT for increasing periods of time (right panels). Samples were run in 1.2% agarose gels containing 1 μM ethidium bromide. Upper panels: Pictures of film negatives under UV transillumination. DNA breaks convert closed circular into nicked DNA (N). Lower panels: Densitometer scanning of gel picture negatives. Percent nicked DNA relative to control was quantified using the formula $100[(N - N_0)/(1 - N_0)]$ where N and N_0 correspond to the fraction of nicked DNA in treated and control samples, respectively.

CPT-induced DNA cleavage in the presence of 365-nm UV light was measured as a function of CPT concentration and irradiation time (Figure 1). Under these conditions, neither UV irradiation nor CPT induced by themselves significant DNA cleavage (not shown).

Sequencing of DNA Cleavage Sites Induced by CPT–UV. CPT-induced DNA photolesions were sequenced within a 254 bp DNA fragment from the human c-myc first intron that had been labeled at one of its 5′ termini. Photocleavage was minimal after 1-h irradiation in the presence of 100 μM CPT (Figure 2). While sample overloading confirmed DNA cleavage (lane 2, panel B), bands were not well-defined. In an attempt to better demonstrate these lesions, photoreacted CPT-treated DNA was subsequently treated with piperidine. Piperidine functions to remove damaged bases and hydrolyze the DNA phosphodiester backbone which allows localization of the lesion. CPT–UV-induced DNA cleavage was enhanced by piperidine treatment (compare lanes 2 and 3, Figure 2). Minimal cleavage was induced by piperidine treatment after UV irradiation in the absence of CPT (lane 1). Comparison between the guanine sequencing (lane 4) and the CPT–UV reactions (lanes 2 and 3) suggests that CPT–UV-induced damage took place only at guanines. Additionally, polyguanine runs were markedly more reactive than isolated guanines. Within the polyguanine runs, cleavage occurred preferentially at the 5′-guanines. The 3′-guanines were the least cleaved in the polyguanine run with an intensity comparable to isolated guanines [compare CPT-induced cleavage at the guanine doublets 3175, 3171, or 3167 with cleavage at the single guanine 3138 (panel B)]. The reactivity of isolated versus consecutive guanines appears clearly in Figure 3 which demonstrates the increased reactivity in polyguanines with photoactivated CPT (solid curve) when compared to dimethyl sulfate (dashed curve).

CPT-Induced Photodamage Occurs Only at Guanines. Piperidine treatment does not reveal all possible DNA lesions. Therefore, primer extension experiments were performed using the 254 bp human c-myc DNA fragment that previously had been reacted with CPT and UV irradiation (Figure 4). Stop points were found only at cytosine incorporation sites, indicating the existence of corresponding lesions at guanines on the template (Figure 4). Single guanines on the template did not induce stop points except for the 6 out of 14 sites that had a 3′-adenine (Figure 5, single G with an asterisk, most of them between 3109 and 3167 positions). In agreement with the piperidine results, the most intense stop points corresponded to the 5′ flank of guanine runs (see lesions at positions 3209, 3216, or 3224; Figure 5).

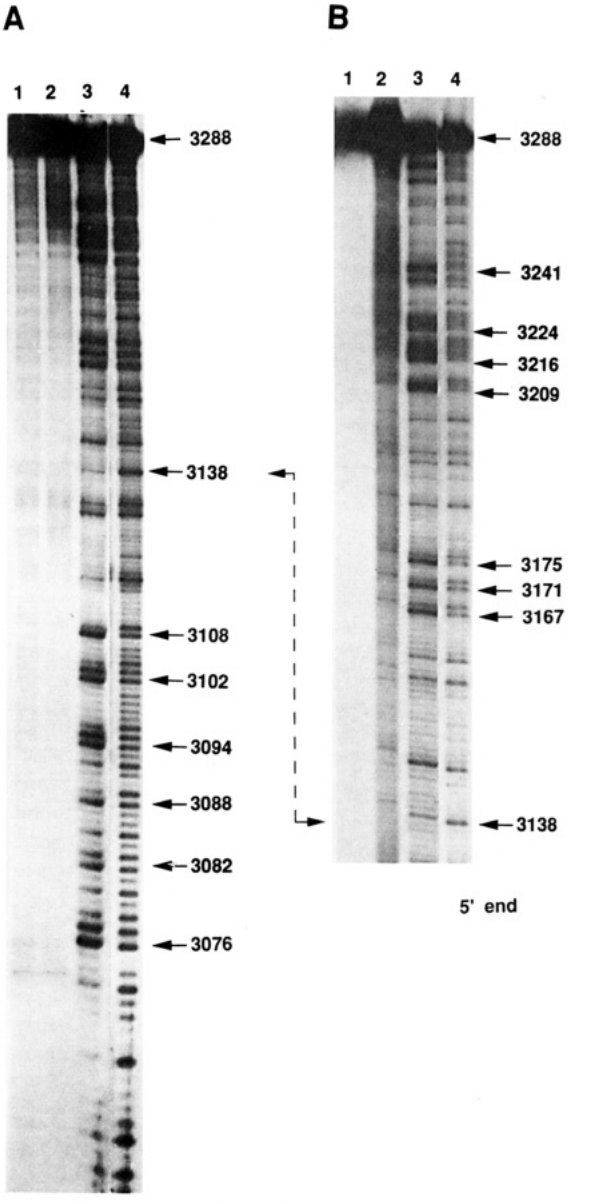

FIGURE 2: Sequencing of CPT-induced photocleavage sites in human c-myc DNA. A 5′-^{32}P-end-labeled 254 bp fragment was exposed to UV light for 1 h, with or without CPT (100 μM), and then treated with hot piperidine (excepted in lanes 2). Electrophoreses were in 8% denaturing polyacrylamide gels. Panel A: Autoradiography of the sequencing gel. Panel B: Same as (A), but from a sequencing gel run further. Lanes 1, UV alone with piperidine; lanes 2, CPT + UV without piperidine; lanes 3, CPT + UV with piperidine; lanes 4, dimethyl sulfate reaction with DNA cleavage at guanines. Arrows and numbers correspond to genomic positions.

CPT-Induced Photodamage in an Oligonucleotide Containing a Strong top1 Site. CPT-induced DNA photolesions were analyzed in a 30-mer oligonucleotide containing a strong CPT-inducible top1 cleavage site originally found in SV40 DNA (Jaxel et al., 1991) (Figure 6). In the duplex oligonucleotide, CPT–UV cleavage was induced at every G, including that flanking the top1 site (arrowhead with asterisk

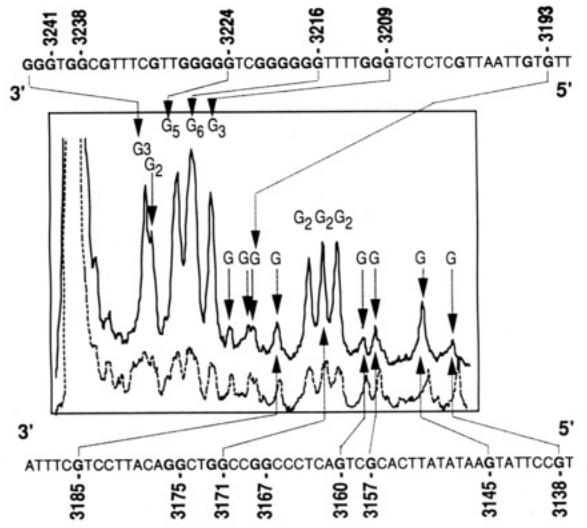

FIGURE 3: Sequence selectivity of CPT-induced photocleavage. Lanes 3 and 4 of the gel shown in Figure 2, panel B, were quantified using a Betascope 603 blot analyzer (Betagen, Waltham, MA). Solid line, 100 μM CPT + UV followed by piperidine; dashed line, dimethyl sulfate reaction followed by piperidine. Numbers correspond to genomic positions.

in Figure 6). In agreement with the results obtained in the human c-myc fragment, CPT-induced DNA photocleavage was markedly enhanced and the band sharpened by piperidine treatment (compare lanes 9 and 10). Single-stranded oligonucleotide was more sensitive than duplex oligonucleotide since the intact oligonucleotide band at the top of the gels was significantly more depleted with the single-stranded than with the double-stranded oligonucleotide (compare lanes 3–4 and 7–8).

Effects of Biochemical Modifiers of CPT-Induced DNA Photolesions. (A) Effect of Excess Mononucleotide Triphosphates. Since CPT-induced DNA photolesions appeared more intense in single- than in double-stranded DNA (see above), CPT reactivity was tested in the presence of mononucleoside triphosphates by competition experiments using approximately 0.1 pmol of the 254 bp human c-myc DNA fragment as a substrate (Figure 7). Dideoxyguanosine triphosphate reduced the intensity of CPT-induced photolesions with almost complete protection at 10 mM and approximately 80% protection at 1 mM (lanes 3 and 4, panel A, Figure 7). In contrast, neither dideoxyadenosine (lanes 5 and 6), nor dideoxycytosine (lane 7), nor dideoxythymidine triphosphates (not shown) had any detectable effect. These results indicate that dideoxyguanosine triphosphate is able to compete, although with a low affinity, with double-stranded DNA for photoactivated CPT, and suggest that photoactivated CPT may react specifically with that nucleotide. Overall, these data show the preferential reactivity of G's with photoactivated CPT. The most reactive G's were in single-stranded DNA, then in double-stranded DNA, and last in the dideoxymononucleotide triphosphate.

(B) Effects of Scavengers. Photoreactions usually result either from free radical or from drug triplet formation. Among the free radical scavengers, thiourea (0.5 mM) was very effective (Figure 7B, lane 3), while mannitol (10 mM) and sodium benzoate (10 mM) were not (Figure 7B, lanes 2 and 4). Catalase (40 units = 100 μg/mL) was also efficient (Figure 7C, lanes 4 and 5), and this effect was related to the catalase enzymatic activity since both heat-inactivated enzyme and albumin were inactive (Figure 7C, lanes 3 and 2). By contrast, superoxide dismutase (8.4 units or 90 μg/mL) was a poor scavenger (Figure 7C, lane 6). Sodium azide (1 mM), which

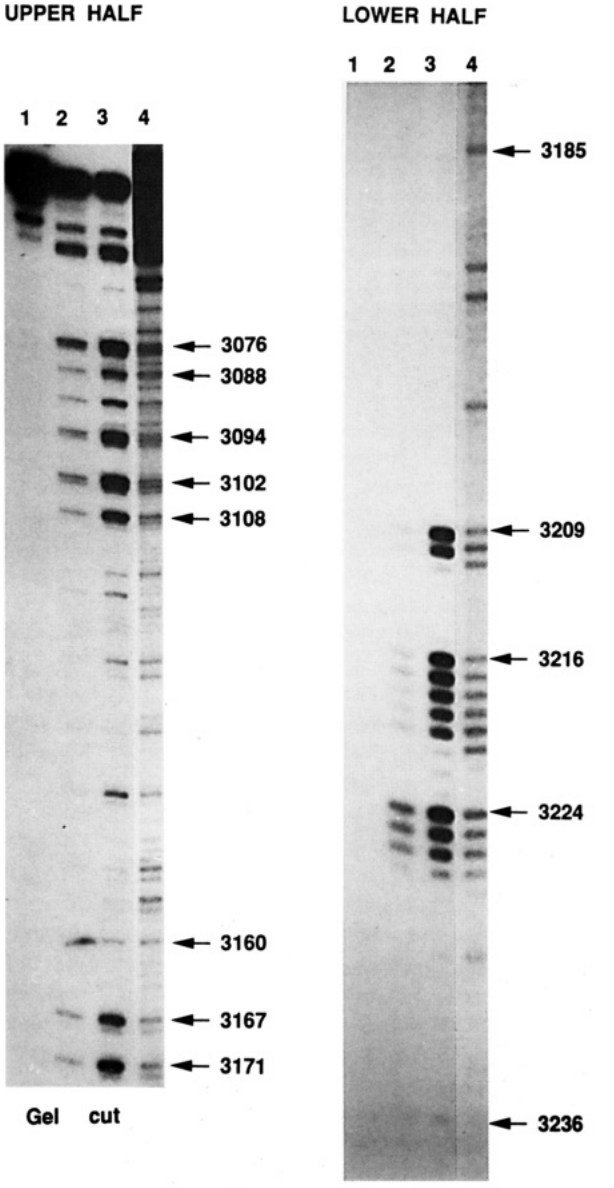

FIGURE 4: Detection of CPT-induced DNA photolesions by primer extension. The same human c-myc DNA fragment as used in Figures 2 and 3 was photoreacted with or without 100 μM CPT, ethanol-precipitated, and then used as template for the extension of a 5'-labeled primer by Taq DNA polymerase. Samples were run in an 8% denaturing polyacrylamide gel. After electrophoresis, the gel was cut in two and autoradiography performed. Lane 1, UV alone; lane 2, CPT + UV for 30 min; lane 3, CPT + UV for 60 min; lane 4, dideoxycytidine sequencing reaction.

is a scavenger of radical singlet and triplet molecules, was also efficient (Figure 7B, lane 5). Finally, removal of dissolved oxygen through argon purge greatly increased photolesions (Figure 7A, lane 8). These results are all consistent with the formation of CPT radicals and/or CPT triplet during photoactivation followed by the appearance of secondary hydrogen peroxide but no hydroxyl radical.

(C) Effect of Cations. To test the proximity of CPT to DNA during CPT photoactivation, various cations were used to alter the potential drug binding to DNA. Mono- and divalent cations, acting as counterions for neutralization of DNA negative charges, are known to attenuate drug binding through steric competition (Hartley et al., 1990; Prakash et al., 1990). Sodium and magnesium chloride decreased CPT-induced photodamage (Figure 7D, lanes 4 and 5). The divalent magnesium cation was more potent than monovalent sodium. The data are consistent with the view that CPT-induced DNA

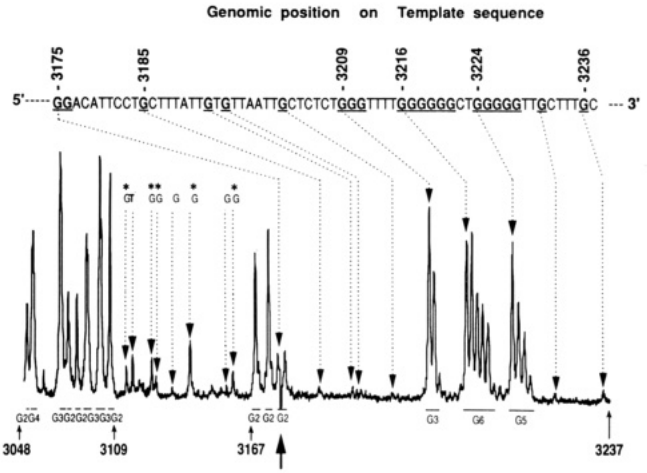

FIGURE 5: Quantitation of CPT-induced DNA photolesions as determined by primer extension. The gel corresponding to Figure 4 was analyzed with a Phosphoimager (Molecular Dynamic, Sunnyvale, CA). The profile of lane 3 is shown. The template sequence is indicated with its guanines enlightened. Single guanines with a 3′-adenine are indicated with a star. The gel cut is indicated with an arrow under the profile. Numbers correspond to genomic positions.

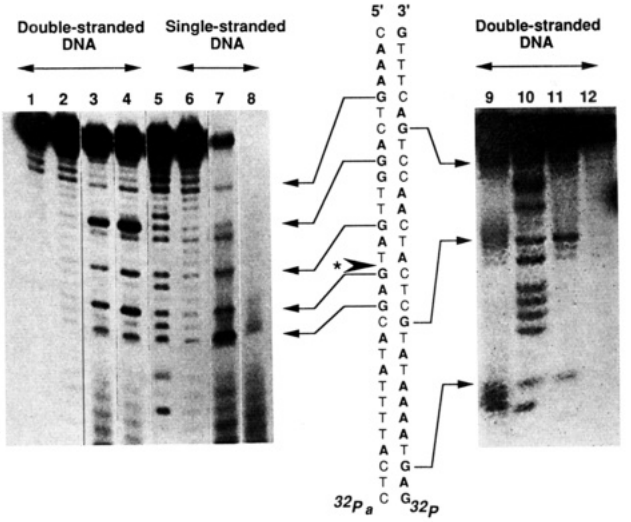

FIGURE 6: CPT-induced DNA cleavage in double- and single-stranded oligonucleotides. A 30-mer oligonucleotide containing a strong top1 site inducible by CPT was used. The star with arrowhead indicates the top1 cleavage site position. Left panel: Cleavage in the strand bearing the potential top1 site. DNA was labeled at the 3′ end with [^{32}P]cordycepin (^{32}P a) and terminal transferase. Lane 1, control DNA treated with piperidine; lanes 2–4, double-stranded oligonucleotide UV-irradiated for 1 h in the presence of 0, 5, and 50 μM CPT, respectively, and then treated with piperidine; lanes 6–8, single-stranded oligonucleotide treated as in lanes 2–4; lane 5, purine sequencing. Right panel: Cleavage in the complementary strand. ^{32}P labeling was at the 5′-DNA terminus. Lane 9, CPT + UV without piperidine; lane 10, purine sequencing; lane 11, CPT + UV followed by piperidine; lane 12, UV alone followed by piperidine. CPT concentration was 50 μM; UV irradiation was for 2 h. Electrophoreses were in 16% denaturing polyacrylamide gels.

photolesions result from activated CPT molecules in the immediate proximity of DNA.

Polyamines like spermine are also polycations that bind to the DNA as counterions and protect DNA against radiation damage (Khan et al., 1992). Besides this nonspecific effect, spermine binds preferentially to the DNA minor groove in AT regions and distorts the DNA helix. Interestingly, in our assay, spermine increased CPT-induced photolesions (Figure 7D, lanes 2 and 3). This effect may result from binding sites in the neighborhood of poly(G) tracks.

DISCUSSION

The present study shows that UVA photoactivation of CPT produces DNA damage. Low-level DNA single-strand breaks were detected using closed-circular SV40 DNA, consistent with previous results (Hertzberg et al., 1989a; Kuwahara et al., 1986; Lown & Chen, 1980). In addition, we demonstrate here that photoactivated CPT produces sequence-selective DNA lesions. Using uniquely end-labeled c-myc DNA fragments, we found that cleavage was enhanced by piperidine treatment at 90 °C and that it was limited to guanines. The GC richness of c-myc DNA enabled us to find that guanine runs were more cleaved than single guanines and that cleavage was most intense at the 5′ end of such runs. Specific guanine lesions were also demonstrated using primer extension in the absence of piperidine treatment. As in the case of hot piperidine treatment, CPT photolesions were most intense on the 5′ side of polyguanine runs.

In previous studies, metals, such as iron and copper, were used to increase the DNA cleavage efficiency of photoactivated drugs (Sakurai et al., 1992). In the presence of copper, CPT photoactivation has been reported to produce essentially random DNA cleavage (Kuwahara et al., 1986), which is probably due to DNA backbone sugar attack by the hydroxyl radical formed, through Fenton-type reactions. Under these conditions, most CPT molecules are photoactivated in solution and react with the solvent (water, solvated oxygen) to generate secondary radicals. To avoid the occurrence of such nonspecific reactions, 0.1 mM EDTA was included in the reactions to reduce the effect of metal traces (Sakurai et al., 1992). In addition, 10 mM Tris buffer instead of phosphate buffer was used (Hicks et al., 1986) to quench radicals generated at a distance from the DNA. These conditions were used to specifically analyze photolesions induced by the drug in contact with the DNA. Under such conditions, CPT-induced photolesions generated only minimal single-stranded cleavage (Figure 1, lanes 2 in Figure 2, and lane 9 in Figure 6).

In the absence of piperidine and heat, preferential cleavage appeared at guanines, but band fuzziness suggested heterogeneous DNA termini at the cleavage sites (see Figures 2 and 6, lanes 2 and 9, respectively). It is well established that most DNA modifications are not directly visible in sequencing gels. Apurinic sites and base damage such as guanine alterations on positions N^7 or C^8 appear clearly on sequencing gels only after hot piperidine treatment which induces base removal and DNA backbone cleavage around the altered base (Maxam & Gilbert, 1980). On the DNA samples reacted with CPT–UV, the piperidine step produced a substantial increase of DNA breaks that were only at guanines (Figures 2 and 6). Similarly, in single-stranded DNA, only guanine lesions were detected, and cleavage was more intense than in double-stranded DNA (Figure 6). This increased reactivity of single-stranded oligonucleotides could be related to the higher reactivity of the latter to radicals (Carmichael et al., 1992). Also, in the competition experiments using free nucleotides, the same preference for dideoxyguanosine triphosphates was observed, although the affinity for these mononucleotides appeared low (Figure 7). These observations suggest specific interactions between photoactivated CPT and guanosines. In addition, the greater reactivity of single-stranded DNA is consistent with the lack of CPT DNA intercalation (Hsiang et al., 1985; Jaxel et al., 1989). Nevertheless, these results do not exclude DNA stacking between CPT and guanosine (Jaxel et al., 1991).

Some DNA lesions, such as purine alkylation on position O^6 or N^3, are not revealed by piperidine treatment. A large excess of DNA lesions over breaks has also been similarly

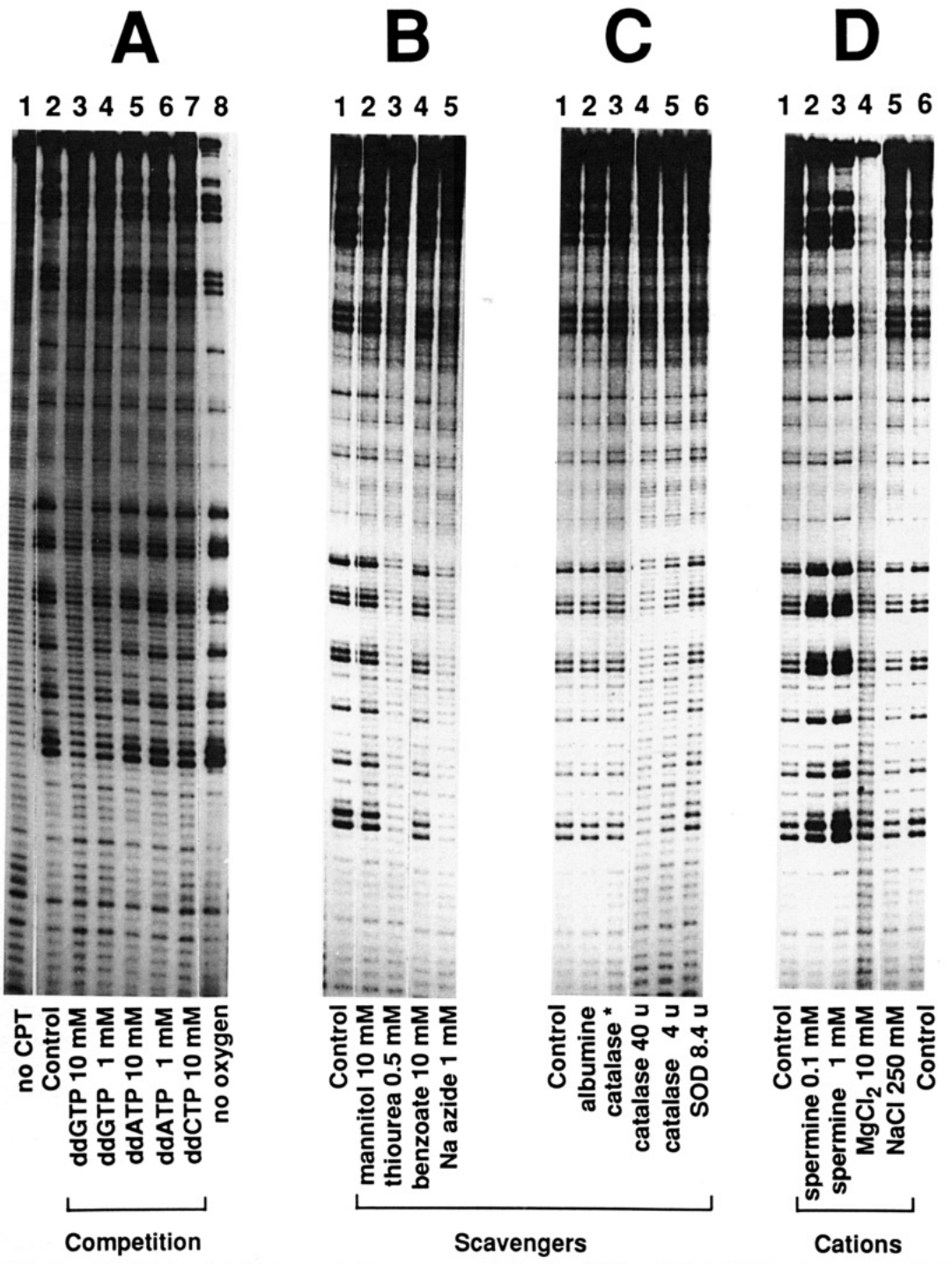

FIGURE 7: Modulation of CPT-induced photocleavage in human c-myc DNA. The 5′-^{32}P-end-labeled 254 bp fragment used in Figures 2 and 3 was exposed to UV light for 2 h in the presence of 100 μM CPT as indicated. Samples were treated with piperidine before electrophoresis in 7% denaturing polyacrylamide gels. Autoradiograms are shown. Panel A: Competition with dideoxynucleotides (ddNTP) and enhancement by oxygen depletion. Lane 1, UV without CPT; lane 2, CPT + UV; lane 3, CPT + UV in the presence of 10 mM ddGTP; lane 4, same with 1 mM ddGTP; lane 5, with 10 mM ddATP; lane 6, with 1 mM ddATP; lane 7, with 10 mM ddCTP; lane 8, CPT + UV treatment was performed after oxygen removal and replacement with argon. Panel B: Effect of chemical radical scavengers. Lane 1, CPT + UV; lane 2, same + 10 mM mannitol; lane 3, +0.5 mM thiourea; lane 4, +10 mM sodium benzoate; lane 5, +1 mM sodium azide. Panel C: Effect of enzymatic radical scavengers. Lane 1, CPT + UV; lane 2, same + 100 μg/mL bovine serum albumin; lane 3, +40 units (100 μg/mL) heat-inactivated catalase (catalase*); lane 4, +40 units of catalase; lane 5, +4 units of catalase; lane 6, +8.4 units (90 μg/mL) superoxide dismutase (SOD). Panel D: Effect of cations. Lanes 1 and 6, CPT + UV; lanes 2 and 3, same + 0.1 and 1 mM spermine, respectively; lane 4, +10 mM $MgCl_2$; lane 5, +250 mM NaCl.

reported for photoactivated methylene blue (Schneider et al., 1990). Therefore, primer extension at 72 °C with Taq polymerase was used to detect DNA lesions more globally in the absence of the piperidine step (Figure 4). Polymerases are usually stopped by bulky DNA adducts such as cisplatin or psoralen adducts (Murray et al., 1992; Sage et al., 1989). With CPT–UV-treated DNA templates, primer extension showed strong and selective stop points corresponding to guanines in the treated DNA template (except one T at position 3120). These stop points were strongest at the 5′ end of polyguanine runs (Figures 4 and 5). Stop points could correspond to breaks and/or lesions on the template. Because of the low number of breaks observed in the absence of hot piperidine, the stop points are likely to represent mainly CPT-induced base photolesions. Therefore, both the hot piperidine and the primer extension methods yielded similar results and

demonstrated that photoactivated CPT induced specific guanine lesions.

The most frequent guanine modifications revealed by a piperidine step involve the N^7 or C^8 positions. Photoactivated CPT, as classical alkylating agents, react preferentially with polyguanines (Figures 4 and 5) (Mattes et al., 1986; Said & Shank, 1991). However, the reactivity of poly(G) was different for photoactivated CPT that react on the 5′ flank than for alkylating agents that react preferentially on the most electronegative guanine N^7 positions lying in the middle of poly(G) (Mattes et al., 1986; Pullman & Pullman, 1981; Said & Shank, 1991). Both photoactivated aflatoxin B_1 and 3-carboxypsoralen give profiles similar to those obtained with photoactivated CPT (Sage et al., 1989; Said & Shank, 1991). The best accessibility on the 5′ edge of polyguanine runs was suggested to explain the polarity. Beside N^7 alkylation, photoactivated aflatoxin B_1 and 3-carboxypsoralen also react with the C^8 guanine position (Sage et al., 1989; Stark et al., 1990). Because nonnucleophile attacks (see below) seem more frequent on C^8 than on N^7 guanine (Augusto et al., 1990; Sharma et al., 1989) and because modifications at the C^8 position are alkali-sensitive and dramatically slow down DNA polymerase at the damaged site (Figure 5) (Shibutani et al., 1991), CPT-induced photolesion on C^8 guanine seems plausible.

The mechanism of the CPT-induced guanine photolesions remains unclear at the present time. It may involve photoaddition such as N^7 or C^8 alkylation, but also photooxidation. The two phenomena probably arise from the same initial step. The photon energy caught by the drug pushes one electron of the drug molecule to a higher electron shell and produces either singlet, triple, or radical forms of the molecule (Cadet et al., 1986; Sage et al., 1989). Sodium azide (Figure 7B), a triplet and radical scavenger, inhibited the CPT-induced photolesions. The increase of CPT-induced photolesions in the absence of oxygen (Figure 7A) is consistent with the results of Lown and co-workers (Lown & Chen, 1980) and with deactivation of the CPT triplet by oxygen (Land et al., 1988). That reaction produces singlet oxygen (reaction type I) (Martin & Burch, 1990). However, significant formation of singlet oxygen was unlikely both because two scavengers of that species, spermine (Khan et al., 1992) and histidine (Lown & Chen, 1980), did not protect from CPT-induced photolesions (Figure 7D) and because the photodamage increased in the absence of oxygen. Therefore, deactivation of the CPT triplet should take place through a type I mechanism (Martin & Burch, 1990). In aerobic conditions, oxygen radicals and peroxides could theoretically be generated. Hydrogen peroxide was produced as suggested by the inhibitory effect of catalase, but only few superoxide anions were generated as suggested by the weak effect of superoxide dismutase (Figure 7C). Among the radical scavengers tested, thiourea was active while mannitol and benzoate were not (Figure 7B). The mannitol inactivity suggests the absence of formation of hydroxyl radicals. Also, the specificity of CPT-induced lesions contrasts with that almost randomly produced by hydroxyl radicals. The scavenging activity of thiourea may be due to its small size, while the inactivity of benzoate may be related to its negative charge that may repel benzoate from DNA and photoactivated CPT. Overall, direct guanine modification by photoactivated CPT is more likely than solvent activation followed by diffusion of secondary oxidant species. Our data are compatible with a mechanism involving either a CPT triplet or a CPT radical. Similar interpretations were obtained from psoralen studies (Boyer et al., 1988).

The requirement of a close contact between guanine and CPT for the production of DNA lesions was further explored. Addition of cations produces a counterion layer that reduces both DNA intercalation and steric access to exogenous molecules (Hartley et al., 1990; Munson et al., 1992). Accordingly, CPT-induced DNA lesions were reduced in the presence of cations. Magnesium was more potent than sodium as previously observed with other molecules such as photoactivated porphyrin or the antitumor antibiotic alkylating agent CC-1065 (Hartley et al., 1990; Munson & Fiel, 1992). Interestingly, for CC-1065, magnesium selectively reduced adenine alkylation from the major groove (at N^7) over alkylation at N^3 from the minor groove (Hartley et al., 1990). The addition of spermine, a physiological polycation, increased CPT lesions. This is consistent with the observations of Lown, who demonstrated an increase of CPT-induced DNA photocleavage in the presence of distamycin, another polycation with minor groove specificity (Lown & Chen, 1980). Opposite effects of cations versus polycations can result from specific alterations of DNA conformation. By occupying the DNA minor groove and reducing its size while increasing the width of the major groove, polyamines may increase major groove accessibility to photoactivted CPT and increase guanine lesions. The increased reactivity of negatively supercoiled versus relaxed DNA may have the same explanation (Lown & Chen, 1980). Hence, major groove accessibility may be an important factor for CPT-induced photolesions.

Our finding that 20-deoxyCPT and CPT lactam, which do not undergo facile E-ring-opening to the camptothecin carboxylate form (Jaxel et al., 1989), were also active at inducing guanine photolesions (result not shown) suggests that the CPT E-ring-opening is not involved in CPT photoactivation. This conclusion is also supported by our additional observation that camptothecin sodium could be photoactivated (data not shown), and is in agreement with the previous structure–activity data of Lown and co-workers (Lown & Chen, 1980; Lown et al., 1981). Therefore, it is possible that CPT photoproducts involve primarily a CPT molecule activated on oxygen 16a as a triplet or as a radical (Lown & Chen, 1980; Lown et al., 1981).

This study provides additional evidence for interaction of the nonintercalator topl inhibitor CPT with DNA and is consistent with the stacking model of CPT with guanines at the 5′ terminus of topl cleavage sites (Jaxel et al., 1991). It is also interesting that two other nonintercalator top2 inhibitors, etoposide and quinolones, have been shown to exhibit better affinity for single- than for double-stranded DNA (Chow et al., 1988; Shen et al., 1989). In the context of topoisomerase reactions, it is possible that the DNA at the cleavage site becomes locally denatured to allow strand passage and that binding of planar drugs, possibly by base stacking, may occur with one of the bases flanking the cleavage site. Steric hindrance may then prevent DNA religation and stabilize cleavable complexes. In the case of CPT, the preferential drug interaction with guanines (this report) combined with the topl requirement for a T–1 at the cleavage site could explain the preferential cleavage pattern between a T and a G (Jaxel et al., 1991).

Specific study of the religation step, using suicide oligonucleotides, strongly suggests that CPT inhibits the religation step (Kjeldsen et al., 1992). Additionally, the base at the 5′ terminus of the cleavage site (usually G for a site stimulated by CPT) might be modified to account for the preferential religation with an external oligonucleotide terminus (Gromova et al., 1993). That modification may involve E-ring-opening of CPT and the formation of a transient covalent intermediate.

E-ring-opening by nucleophilic attack on C-21 may play an essential role in the interaction of camptothecin with topl-linked DNA breaks since the lactone structure and the 20-hydroxyl are necessary for topl inhibition (Jaxel et al., 1989; Hertzberg et al., 1989b; Pommier & Tanizawa, 1993). The nucleophilic attack may involve a topl amino acid (serine hydroxyl, cysteine sulfhydryl, histidine imidazole, etc.) or a DNA base. Reversibility of camptothecin-induced topl-linked DNA breaks may be facilitated by intramolecular attack of the C-17 primary alcohol on the electrophilic C-21 carbonyl (Adamovics & Hutchinson, 1979; Kingsbury et al., 1991).

DNA binding of topoisomerase I and II inhibitors acting through stabilization of the cleavable complex seems to be a necessary step of the reaction, even with a low affinity, since all the classical nonintercalator inhibitors, epipodophyllotoxins (Chow et al., 1988), quinolones (Shen et al., 1989), and CPT (Fukada, 1985; this work), have been shown to interact with the DNA. Finally, this work suggests an interaction of the inhibitors, CPT in the present case, with specific bases. This base specificity, compatible with the stacking model, could explain the specific cleavage pattern obtained with different topoisomerase inhibitors (Pommier et al., 1993).

ACKNOWLEDGMENT

We thank Dr. Joseph Barchi and Dr. Vincent Favaudon for helpful discussions and Dr. Kenneth Kraemer for his technical support and valuable discussion.

REFERENCES

Adamovics, J. A., & Hutchinson, C. R. (1979) *J. Med. Chem. 22*, 310–314.

Augusto, O., Cavalieri, E., Rogan, E., RamaKrishna, N., & Kolar, C. (1990) *J. Biol. Chem. 265*, 22093–22096.

Boyer, V., Sage, E., & Moustacchi, E. (1988) *Biochemistry 27*, 3011–3018.

Cadet, J., Berger, M., Decarroz, C., Wagner, J. R., Van Lier, J. E., Ginot, Y. M., & Vigny, P. (1986) *Biochimie 68*, 813–834.

Capranico, G., Kohn, K. W., & Pommier, Y. (1990) *Nucleic Acids Res. 18*, 6611–6619.

Carmichael, P. L., Ni Shé, M., & Phillips, D. H. (1992) *Carcinogenesis 13*, 1127–1135.

Champoux, J. (1990) in *DNA topology and its biological effects* (Wang, J. C., & Cozarelli, N. R., Eds.) pp 217–242, Cold Spring Harbor Laboratory, Cold Spring Harbor, NY.

Chow, K. C., Macdonald, T. L., & Ross, W. (1988) *Mol. Pharmacol. 34*, 467–473.

Fosse, P., Rene, B., Le Bret, M., Paoletti, C., & Saucier, J.-M. (1991) *Nucleic Acids Res. 19*, 2861–2868.

Fukada, M. (1985) *Biochem. Pharmacol. 34*, 1225–1230.

Gromova, I., Kjeldsen, E., Svejstrup, J., Alsner, J., Christiansen, K., & Westergaard, O. (1993) *Nucleic Acids Res. 21*, 593–600.

Hartley, J. A., Forrow, S. M., & Souhami, R. L. (1990) *Biochemistry 29*, 2985–2991.

Hertzberg, R. P., Caranfa, M. J., & Hecht, S. M. (1989a) *Biochemistry 28*, 4629–4638.

Hertzberg, R. P., Caranfa, M. J., Holden, K. G., Jakas, D. R., Gallagher, G., Mattern, M. R., Mong, S. M., Bartus, J. O., Johnson, R. K., & Kingsbury, W. D. (1989b) *J. Med. Chem. 32*, 715–720.

Hertzberg, R. P., Busby, R. W., Caranfa, M. J., Holden, K. G., Johnson, R. K., Hecht, S. M., & Kingsbury, W. D. (1990) *J. Biol. Chem. 265*, 19287–19295.

Hicks, M., & Gebicki, J. M. (1986) *FEBS Lett. 199*, 92–94.

Hsiang, Y. H., Hertzberg, R., Hecht, S., & Liu, L. F. (1985) *J. Biol. Chem. 260*, 14873–14878.

Jaxel, C., Kohn, K. W., Wani, M. C., Wall, M. E., & Pommier, Y. (1989) *Cancer Res. 49*, 1465–1469.

Jaxel, J., Capranico, G., Kerrigan, D., Kohn, K., & Pommier, Y. (1991) *J. Biol. Chem. 266*, 20418–20423.

Khan, A., Di Mascio, P., Mereidos, M., & Wilson, T. (1992) *Proc. Natl. Acad. Sci. U.S.A. 89*, 11428–11430.

Kingsbury, W. D., Boehm, J. C., Jakas, D. R., Holden, K. G., Hecht, S. M., Gallagher, G., Caranfa, M. J., McCabe, F., Faucette, L. F., Johnson, R. K., & Hertzberg, R. P. (1991) *J. Med. Chem. 34*, 98–107.

Kjeldsen, E., Svejstrup, J., Gromova, I., Alsner, J., & Westergaard, O. (1992) *J. Mol. Biol. 228*, 1025–1030.

Kuwahara, J., Suzuki, T., Funakoshi, K., & Sugiara, Y. (1986) *Biochemistry 25*, 1216–1221.

Land, E., McLean, A., & Truscott, T. (1988) in *Photosensitisation* (Morena, G., Ed.) H15, pp 69–72, Springer-Verlag, Berlin, Heidelberg, Germany.

Liu, L. F. (1989) *Annu. Rev. Biochem. 58*, 351–375.

Lown, J. W., & Chen, H.-H. (1980) *Biochem. Pharmacol. 29*, 905–915.

Lown, J. W., Chen, H. H., & Planbeck, J. A. (1981) *Chem.-Biol. Interact. 35*, 55–70.

Martin, J. P., & Burch, P. (1990) *Methods Enzymol. 186*, 635–645.

Mattes, W., Hartley, J., & Kohn, K. (1986) *Nucleic Acids Res. 14*, 2971–2987.

Maxam, A., & Gilbert, W. (1980) *Methods Enzymol. 65*, 499–560.

Munson, B. R., & Fiel, R. J. (1992) *Nucleic Acids Res. 20*, 1315–1319.

Murray, V., Motyka, H., England, P., Wickham, G., Lee, H., Denny, W., & McFadyen, D. (1992) *Biochemistry 31*, 11812–11817.

Pommier, Y., & Kohn, K. W. (1989) in *Developments in Cancer Chemotherapy* (Gazer, R. I., Ed.) Vol. 2, pp 175–196, CRC Press, Inc., Boca Raton, FL.

Pommier, Y., & Tanizawa, A. (1993) in *Cancer Chemotherapy* (Hickman, J., & Trittom, T., Eds.) pp 214–250, Blackwell Scientific Publications Ltd., Oxford, U.K.

Pommier, Y., Capranico, G., Orr, A., & Kohn, K. W. (1991) *Nucleic Acids Res. 19*, 5973–5980.

Pommier, Y., Kohn, K. W., Capranico, G., & Jaxel, C. (1993) in *Molecular Biology of DNA Topoisomerases and its Application to Chemotherapy* (Andoh, T., Ikeda, H., & Oguro, M., Eds.) pp 215–227, CRC Press, Boca Raton, FL.

Prakash, A. S., Denny, W. A., Gourdie, T. A., Valu, K. K., Woodgate, P. D., & Wakelin, L. P. (1990) *Biochemistry 29*, 9799–9807.

Pullman, A., & Pullman, B. (1981) *Q. Rev. Biophys. 14*, 289–380.

Sage, E., & Moustacchi, E. (1987) *Biochemistry 26*, 3307–3314.

Sage, E., Le Doan, T., Boyer, V., Helland, D., Kittler, L., Helene, C., & Moustacchi, E. (1989) *J. Mol. Biol. 209*, 297–314.

Said, B., & Shank, R. C. (1991) *Nucleic Acids Res. 19*, 1311–1316.

Sakurai, H., Miki, T., Imakura, Y., Shibuya, M., & Lee, K. H. (1992) *Mol. Pharmacol. 40*, 965–973.

Schneider, J. E., Price, S., Maidt, L., Gutteridge, J. M. C., & Floyd, R. A. (1990) *Nucleic Acids Res. 18*, 631–635.

Sharma, N., Davies, J., Phillips, D., & McCloskey, J. (1989) *Nucleic Acids Res. 17*, 955–967.

Shaulsky, G., Johnson, R. L., Shockcor, J. P., Taylor, L. C., & Stark, A. A. (1990) *Carcinogenesis 11*, 519–527.

Shen, L., Baranowski, J., & Pernet, A. (1989) *Biochemistry 28*, 3879–3885.

Shibutani, S., Takeshita, M., & Grollman, A. (1991) *Nature 349*, 431–434.

Shiraki, T., & Sugiura, Y. (1990) *Biochemistry 29*, 9795–9798.

Stark, A. A., Gal, Y., & Shaulsky, G. (1990) *Carcinogenesis 11*, 529–534.

Wang, J. C. (1991) *J. Biol. Chem. 266*, 6659–6662.